Tissue temperature monitoring during interstitial photodynamic therapy

Jenny Svensson[1], Ann Johansson[1], Nazila Yavari[1,2], Katarina Svanberg[3], Stefan Andersson-Engels[1]

[1]Lund University Medical Laser Centre, Department of Physics, Lund, Sweden.
[2]University of Bergen, Department of Physics and Technology, Bergen, Norway.
[3]Lund University Hospital, Department of Oncology, Lund, Sweden.

Abstract

During δ-aminolevulinic acid based interstitial photodynamic therapy, a high light fluence rate is present close to the source fibers. This might induce an unintentional tissue temperature increase of importance for the treatment outcome. A system to measure the local tissue temperature at the source fibers during interstitial photodynamic therapy on tissue phantoms is presented. The temperature was measured by acquiring the fluorescence from small Cr^{3+}-doped crystals attached to the tip of the illumination fiber used in an interstitial photodynamic therapy -system. The fluorescence of alexandrite crystal is temperature dependent. A ratio between the fluorescence intensities at two different wavelength bands in the red region was used as a measure on the local temperature. The system was calibrated by immersing the fibers in an intralipid solution placed in a temperature controlled oven. Measurements were then performed by placing the fibers interstitially in a pork chop as a tissue phantom. Measurements were also performed superficially on skin on a volunteer. A simulated treatment was conducted for 10 minutes, and the fluorescence was measured each minute during the illumination. The fluorescence yielded the temperature at the fiber tip by the use of the calibration curve. The measurements indicate a temperature increase of a few degrees during the simulated treatment.

Keywords: interstitial photodynamic therapy, temperature-dependent fluorescence, Cr^{3+}-ions

1. Introduction

Fluorescence photodetection and photodynamic therapy (PDT) are techniques currently under clinical assessment for visualization and local destruction of malignant tumors as well as premalignant lesions[1]. PDT is based on a photochemical reaction in presence of oxygen molecules[2,3]. A photosensitizing drug is administrated orally, topically or intravenously, and is selectively accumulated in the tumor to a higher degree than the surrounding normal tissue. The photosensitizer is usually activated by laser light, wavelength-matched to the absorption peak of the photosensitizer. The excited photosensitizer transfers its energy to the surrounding oxygen molecules[4,5], generating singlet state oxygen, which in turn causes tissue oxidation and destruction of the tumor[6,7]. Besides being a minimally invasive modality, the main advantages of PDT are the

selectivity, the smooth and rapid healing and the ability of repeating the treatment on the same area, if necessary[8,9]. The major disadvantage of PDT is the limitation to treat only thin (<3mm) superficial lesions or lesions accessible through body cavities, due to the poor light penetration through the tissue.

One way to slightly overcome this limitation is to use sensitizers with high absorption in the near IR-wavelength range, since the penetration of light in tissue is better in this wavelength region[10], and/or employing a more potent photosensitizer[11]. However, still the treatment depth will not be more than 3-7 mm[12].

An alternative to normal PDT with surface illumination especially for treating thicker or embedded tumors is to utilize optical fibers inserted into the tumor[13]. This method is called interstitial photodynamic therapy (IPDT)[14,15]. In IPDT light is guided into the tumor mass. This enables a selective local treatment[16-18]. There are many treatment situations of deep-lying lesions, where IPDT may be the treatment of choice, hence a number of investigations have been performed employing interstitial light delivery to the tumor[15,19,20]. There are many factors apart from the light fluence affecting the efficacy of PDT/IPDT; such as skin permeability and drug diffusivity (in topically applications of the drug), pH, temperature, oxygenation, photobleaching, enzyme activity, anaesthesia effects, etc. These should all be taken into consideration in the treatment planning. The major aim of the presented study is, among all these factors, to measure the local tissue temperature during PDT.

Many laser applications in medicine produce heat-inducing changes of the tissue, leading to alterations in the optical properties of the tissue[21]. Such alterations will result in redistribution of light within the tissue, and in particular, the penetration of the light within the tissue may be reduced[21]. The absorbed optical energy generates heat, which also can act synergistically with PDT[22]. Normally the power density of the treatment light when employing surface illumination is low enough not to cause any significantly increased tissue temperature. It has, however, been discussed that hyperthermic cell killing (temperature $\geq$ 44°C) may be important for surface irradiance at high fluence rates. The role of irradiation-induced temperature rises may be more important in IPDT. Presence of a high light fluence rate nearby the source fiber, especially for bare end clear cut fiber light delivery, might increase the tissue temperature significantly, and hence affect the treatment results[13,23].

A number of optical techniques are developed for diagnostic purposes. One such technique is laser-induced fluorescence (LIF). A motivation for utilizing LIF for the diagnosis of tissue pathologies is that fluorescence is sensitive to the biochemical composition of the tissue[24]. Fluorescence techniques can also be utilized to monitor the photosensitizer concentration in PDT or IPDT[25]. Tissue fluorescence spectroscopy is usually performed using optical fibers. The excitation light is guided through an optical fiber probe, and the tissue fluorescence is detected through the same or another fiber. The detected fluorescence signals depend, however, not solely on the fluorophore content, but are also affected by the tissue optical properties and the geometry of the measurement. One thus needs to consider the measurement geometry and optical properties of tissue in the analysis of the signals.

An instrument for IPDT has been developed by the company SpectraCure AB (Ideon Research Park, Lund, Sweden) for light delivery through a multiple fiber arrangement[18]. In

this instrument the fibers used for light delivery are also utilized in other modes for measuring the delivered light dose, for monitoring the drug-related fluorescence and the oxygen content in the tissue. During an IPDT treatment procedure a high light fluence rate is present close to the source fibers, especially when using bare end cut fibers[13]. This might induce an unintentional tissue temperature increase of importance for the treatment outcome. In addition, an increase in the measured absorption coefficient has been seen during IPDT treatments in a recent study[13]. The increase in the absorption coefficient could be an effect of tissue deoxygenation, changes in blood flow, and local bleeding. These alternations may be induced by the photodynamic or a thermal effect.

The goal of an IPDT treatment is not to have a hyperthermal, but a photochemical effect, of the lesion. If a small bleeding occurs at the fiber tip, the absorption coefficient will increase drastically and this could lead to an abrupt temperature increase. Such bleeding would reduce the efficacy of the treatment, since most of the light would be absorbed in the blood right at the fiber tip. In an earlier published study, the blood perfusion and the temperature were measured during superficial PDT, both on patients with lesions and on skin on volunteers[26]. The temperature was studied with an infrared camera, and a 1-4 °C increase in temperature could be seen during the treatment. This small temperature increase suggests that there is no hypothermal effect during the treatment when the initial skin temperature is about 35 °C. The infrared camera, however, only monitors the temperature of the really superficial layer of the skin, while in deeper lying tissue the temperature could actually be higher.

In this study an optical technique based on optical fiber doped with alexandrite crystal was employed to measure the tissue temperature at the fiber tips during IPDT. Alexandrite, which is the common name for chromium-doped chrysoberyl, Cr^{+3}: $BeAl_2O_4$, is a very special crystal with thermo-mechanical properties enabling temperature measurements with accuracy around the body temperature[27,28]. The special properties of this crystal have given name to a special effect – the alexandrite effect. This is the property of a solid to change its apparent colour when viewed under different commonly-observed "white" light sources. The effect is best known in alexandrite that appears green in sunlight or fluorescent light, and red in incandescent or candle light. There are other materials known that can show an alexandrite effect, such as certain other crystals doped with e.g. Cr^{3+}; Sm^{2+} [29]. The optical-physiological causes of the alexandrite effect have been discussed by several authors[29,30]. The effect is due to a substance having optical absorption bands that are close to critical wavelength boundaries that determine a person's perception of different colors[31]. In addition to its broad absorption bands throughout the visible spectrum, alexandrite exhibits narrow R-line absorption features at wavelengths near 680 nm[27].

The aim of this study is to present results of an optical method to monitor tissue temperatures during simulated treatments superficially on skin (PDT), but also interstitial illumination in a piece of meat (IPDT). In addition, the role of scattering coefficient variation on the detected fluorescence intensity has been investigated by use of different intralipid concentration. Also the effects of illumination-collection fibers separation, together with the changes of the source power, have been investigated.

2. Materials and methods

One way to measure the temperature with an optical technique is to use crystals with temperature dependent fluorescence properties. By attaching a small crystal to the tip of an optical fiber it is possible to measure the temperature in the region of the fiber tip. In this study a crystal doped with Cr^{3+}-ions was used. Cr^{3+}-ions in ionic crystals interact strongly with the crystal field and the lattice vibrations. The interaction between the Cr^{3+}-ions and the crystal field is very high due to the fact that there are no outer shells to shield the three valence electrons. As a result, Cr^{3+}-activated materials are characterised by a wide absorption spectrum, from the UV to the near infrared region.

This has two advantages, the possibility to choose excitation source, and that a small drift in the excitation source will not cause a significant change in the fluorescence intensity. Because of the strong crystal field interaction, the energy gaps of the electronic levels of Cr^{3+} can vary from one host crystal to another. The temperature dependence of the fluorescence properties varies with the energy gap, and will thus differ for different Cr^{3+}-doped crystals. Among the different crystals, alexandrite seems to exhibit good temperature sensitivity in the temperature range (15 – 100 °C), of special interest for the present application.[32]

A Jablonsky diagram of alexandrite is shown in Figure 1. The ground state in Cr^{3+} is always $^4A_2$, independent of the strength of the crystal field. In this study, we employed 635 nm light for excitation. Two excited energy levels were involved, following such excitation: $^4T_2$ and ^2E. The energy splitting between these two states is denoted $\Delta E = E(^4T_2) - E(^2E)$. ΔE varies strongly with the strength of the crystal field and can be both negative and positive.

The emission spectrum of Cr^{3+} consists of two different features, a broad spectral band and two sharp peaks, so called R-lines. The broad band originates from the vibrational transitions, $^4T_2 \rightarrow {}^4A_2$, where ions in the $^4T_2$ state decay to the empty vibrational levels of the $^4A_2$ state. The R-lines appear because of a further split of the ^2E state into two levels, E and $2\bar{A}$, separated by a small energy gap. The R_1-line is the transition $E \rightarrow {}^4A_2$, and the R_2-line comes from the transition $2\bar{A} \rightarrow {}^4A_2$[32]. Lattice vibrations in the crystal interact with the electronic levels of the Cr^{3+}-ion. These result in the initiation of vibrational transitions, radiationless transitions and phonon scattering. The first of these effects produces broad bands in the spectra, the second effect leads to a temperature dependent decrease of the fluorescence lifetimes of the R-lines, and both the second and third effect can cause a thermal broadening of the R-lines[33].

In alexandrite, the lowest excited state of the Cr^{3+}-ions is the ^2E state (Figure 1). At low temperatures the emission is dominated by the transition $^2E \rightarrow {}^4A_2$ (the R-lines), yielding an effective long fluorescence lifetime, since the transition is parity and spin forbidden. The $^4T_2$ state has a much shorter lifetime than the ^2E state. When the temperature increases, a higher percentage of the Cr^{3+}-ions will populate the $^4T_2$ state according to the Boltzmann distribution. Consequently, more ions will decay through the $^4T_2 \rightarrow {}^4A_2$ path, resulting in a broad emission and a decrease of the fluorescence lifetime. Thus, at low temperatures, the thermally activated populations of the ^2E and $^4T_2$ states determine the fluorescence properties[32]. This phenomenon can also be seen in the intensity of the fluorescence. The fluorescence, corresponding to the R-lines, will decrease when less ions will follow the path $^2E \rightarrow {}^4A_2$. This can be used as a measure of the temperature by

forming a dimensionless ratio for the intensities from the R-lines divided by the intensity at longer wavelengths.

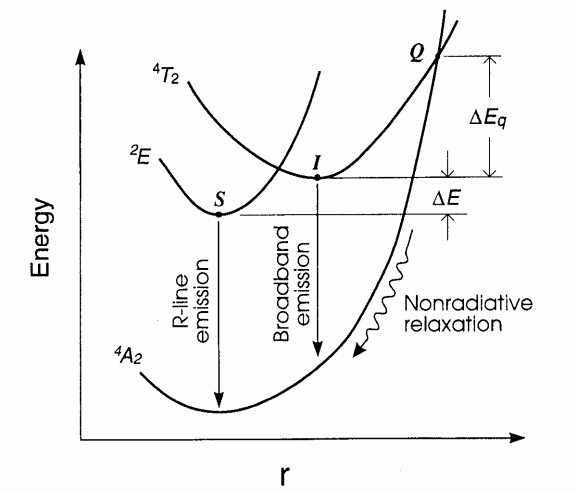

Figure 1. *The energy levels as a function of nearest neighbour distance for a crystal with a high crystal field strength, taken from Ref*[32].

An evaluation of the method measuring the temperature with fluorescence from crystals has been reported earlier[34]. In that study, fluorescence lifetime measurements were performed. There are also commercially available fiber based thermometers using optical techniques to measure temperature dependent fluorescence[35].

In this study, we went one step further, and used an integrated system developed for IPDT to measure the fluorescence and employ a ratio of the intensities at two fluorescence bands as a measure of the actual temperature. A crystal was located on the fiber tip of the fiber delivering the treatment light.

2.1 IPDT system

An instrument for IPDT has been developed by the company SpectraCure AB (Ideon Research Park, Lund, Sweden). A general schematic drawing of the instrument is shown in Figure 2. The instrument uses a maximum of six bare end optical fibers that are used to deliver the therapeutic light into the tumor mass. The same fibers can also be used in order to perform diagnostic measurements during the treatment session[13]. The therapeutic light unit consists of six diode lasers emitting at 635 nm with an individual maximum output power of 200 mW. While in treatment mode, light from the therapeutic light unit is guided into the light distribution module and further coupled into the six 400 μm diameter fibers, which deliver the light to the target tissue.

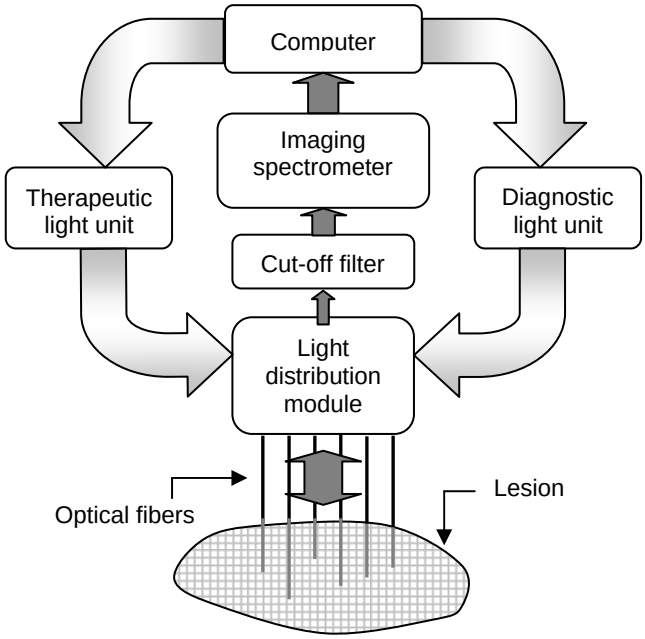

Figure 2. *A schematic description of the IPDT system employed in this study. Modified from Ref*[13] *.*

In the measurement mode, light from the diagnostic light unit is coupled into one of the "patient fibers" via the light distribution module. After interacting with the sample the fluorescence light is collected by the other fibers, and coupled into an imaging spectrometer covering the spectral range between 620 and 810 nm. A cut-off filter (Schott RG665) is used to attenuate the intense laser light at 635 nm from the laser light source. Wavelength calibration of the spectrometer is carried out using an HgAr lamp to determine the relation between wavelength and pixel number in the horizontal direction of the CCD chip[13].

2.2 Temperature Calibration

For the measurements, an end cut fiber with a core diameter of 400 μm (Fiberguide Industries, USA), was used. A small alexandrite crystal was glued to the clear-cut fiber tip, using the glue (Nordland Optical Adhesive 68, Norland Products) that needed to cure in UV-light for 30 minutes. The set-up used for temperature calibration, is shown in Figure 3. The calibration was performed in the temperature interval 15 – 50 °C. Two fibers were immersed in a 1.28 % intralipid mixture (mixed with water). The distance between the fibers was approximately 12 mm. One fiber (fiber 1) was used only for delivering the excitation light and the other one, with an attached piece of crystal (fiber 2), was used for detection of induced fluorescence light. The vessel and the fibers were placed inside a temperature controlled oven (FN300 Nüve Microprocessor). Two thermistors were also placed in the vessel, close to the fibers, to monitor the actual temperature of the intralipid. Once the temperature was stabilized in the intralipid after approximately 45 minutes, the IPDT laser light was switched on and guided through fiber 1. A fluorescence spectrum was recorded. The temperature of the oven was then altered and the temperature was stabilized before the next measurement. This was repeated for temperatures between 15 and 50 degrees (°C). In order to monitor the influences of the power on the detected

fluorescence light, two different powers (90 mW and 130 mW) of the laser light were used for each temperature.

To investigate the influence of different scattering coefficients, calibration measurements were performed for a few different intralipid concentrations.

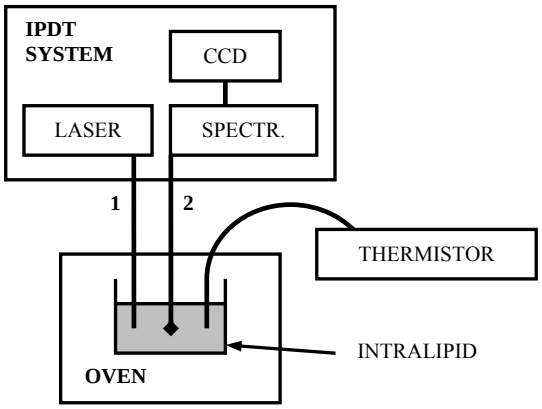

Figure 3. *The arrangement used for the calibration. The fiber used for illumination of the laser light (denoted 1) and the fiber with a piece of crystal (denoted 2) are shown.*

The evaluation of the temperature was performed by using the concept of forming a dimensionless ratio. Integration was made for the intensities in two different wavelength bands, marked with Area 1 and Area 2 in Figure 4, respectively. A ratio was then formed between the two values.

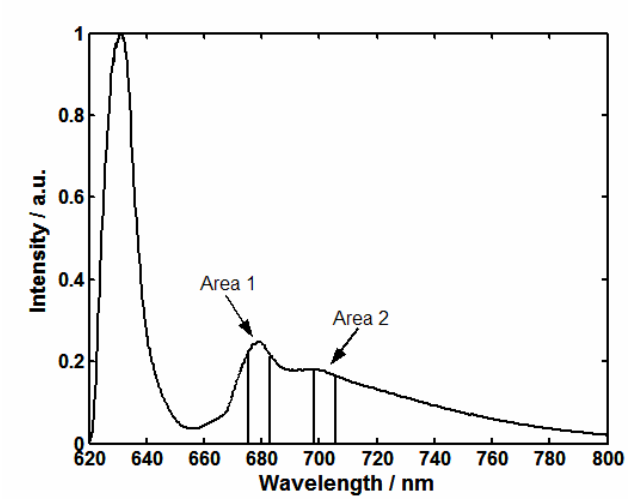

Figure 4. *A fluorescence spectrum from alexandrite indicating the wavelength bands at 680 and 700 nm used for forming a ratio.*

2.3 Experimental arrangements

For the experiments performed in this study, two different arrangements of the two fibers were used. In arrangement A shown in Figure 5a, the end cut fiber, denoted as 1, was used

for illumination during the simulated treatment. The other fiber, denoted as 2, with a crystal attached to the fiber tip, was used to monitor the temperature. The treatment light was used to induce fluorescence in the crystal. The fluorescence light was guided through the fiber into the detection unit in the IPDT system. With this arrangement the temperature was monitored in the spot where the doped fiber was placed, which means a small distance from the treatment fiber.

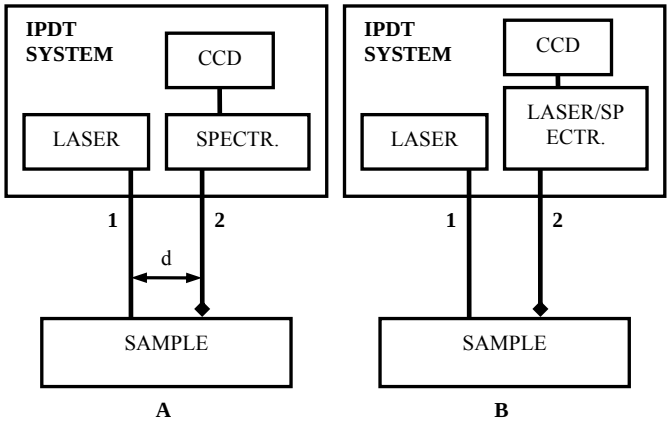

Figure 5. *Two different arrangements of the fibers are shown. In A, the illumination fiber is denoted 1, and the detection fiber with the crystal is marked 2. In the arrangement B, the illumination fiber is the doped fiber (2), measuring the temperature in the same spot where the treatment takes place. The fiber, denoted 1, in B, is only used for inducing fluorescence in the crystal when a temperature measurement is performed.*

In fiber arrangement B, Figure 5b, the fiber with a piece of crystal attached to the tip denoted as 2, was used for illumination during the treatment. This fiber was illuminating the whole time except during the temperature measurements, when it was used for detection of fluorescence light. The tip of the other fiber, denoted as 1, was placed approximately 2 mm from the tip of the first fiber. Fiber 1 was only illuminating during the temperature measurements to induce the fluorescence in the crystal at the other fiber tip. With this set-up the temperature is monitored in the position of the illumination fiber and not at a small distance as in arrangement A. With this arrangement it is, however, not possible to perform any measurements during the treatment irradiation.

2.3.1 Simulation of a contact treatment of skin

Both fiber arrangements were used for the investigation on skin. With arrangement A, the two fibers were placed in close contact with the skin on the arm of healthy volunteer. In the first measurement, a power of 130 mW through the illumination fiber was used, and detection of fluorescence light, with the doped fiber, was performed each 10 seconds during 2 minutes. This was done to see how the temperature changes in the beginning of the illumination period. In the following measurements, two different interfiber distances, 1 and 3 mm, were used. The power from the illumination fiber was measured to 130 mW and the illumination was continued during 10 minutes. A fluorescence measurement was acquired each minute. The temperature of a larger area of the skin was monitored using a calibrated infrared camera (AGEMA 570 Elite, Flir Systems Inc.), which was saving a temperature image every minute.

In the experiment using fiber arrangement B, two different powers, 75 mW and 110 mW, were used for illumination, in order to monitor how the temperature changes as a result of different illumination power. The initial temperature was measured before the treatment. The treatment started by illuminating with the doped fiber (denoted as 2 in Figure 5b). After 1 minute, the treatment light was temporarily interrupted, and the light source to the other fiber (denoted as 1 in Figure 5b) was turned on. Detection of induced fluorescence light from the crystal was performed through fiber 2. The illumination was continued as before, and a temperature measurement was recorded each minute during the treatment. After 10 minutes, the treatment was interrupted, but the measurements continued for a few minutes to study the temperature changes without any illumination.

2.3.2 Simulation of an interstitial treatment in meat

In the final experiments, interstitial measurements were performed using a pork-chop as a tissue phantom. The two fibers were placed next to each other inside the meat. By using fiber arrangement A in Figure 5, a 10 minutes treatment was simulated. In this case, the output power from the illumination fiber was 130 mW, and the depth of the fibers in the meat was approximately 12 mm. Two experiments were also conducted with arrangement B. In the first experiment, the depth of the fibers was 18 mm with a power of 110 mW. The treatment continued during 20 minutes. In the last experiment the fibers were placed at a depth of 10 mm with a power of 110 mW, but only for 10 minutes. The temperature measurement was performed every minute.

3. Results and discussion

The temperature calibration curve from intralipid in the oven is shown in Figure 6. The curve has been plotted as the ratio of the fluorescence intensities at 680 and 700 nm as a function of the temperature of the thermistor close to the detection fiber for different oven temperatures. The results from both light powers are included. It can be seen that the influence of the light power is very weak, meaning that the laser power did not significantly increase the temperature of the intralipid. Tests were also performed when the distance between the fibers and the scattering properties of intralipid phantoms were changed. The results, not presented here, show that the distance, between the illumination and detection fiber does not influence the fluorescence ratio significantly as long as the signal-to-noise ratio is sufficiently good to evaluate the ratio. These results was expected according to the previous studies[36]. Changes in the scattering properties of the intralipid phantom did not affect the ratio either.

As it is seen from Figure 6, a quadratic polynomial was fitted to the acquired data points. This curve was later used as a calibration curve for determining the temperature measured during the tissue measurements.

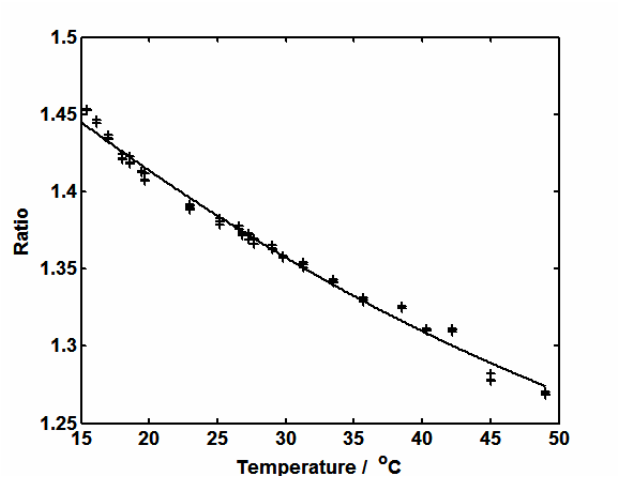

Figure 6. *A calibration curve for the fiber with an attached crystal is shown. Measured values (crosses) and the fitted calibration curve (solid line) to these values are shown.*

From Figure 7, the absolute evaluated temperature as a function of time can be seen at a small distance from the illumination fiber during a two minutes long irradiation session on skin. A quadratic polynomial has been fitted to the measured values. It is seen that the temperature is increasing during the first two minutes and it is stabilizing at later times.

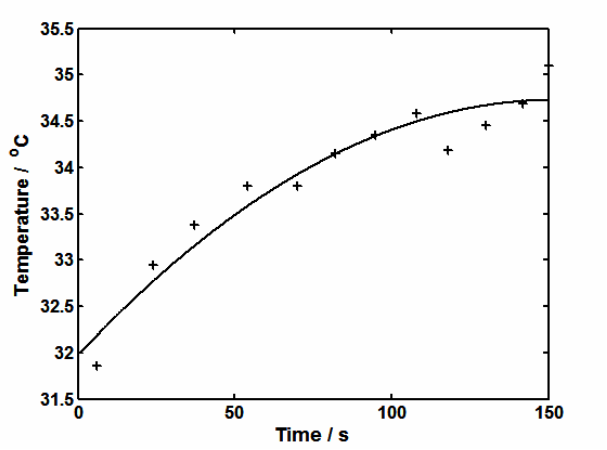

Figure 7. *The temperature increase during the first two minutes of irradiation of the skin of a healthy volunteer is plotted. Measured temperatures (crosses) and a fitted line to the measured values are shown.*

The temperature increase can be seen in Figure 8 as a function of time for two different interfiber distances between the illumination and the doped detection fiber. By changing the distance between the two fibers, the temperature at different distances from the position of the irradiation has been monitored. It is seen the temperature is higher close to the irradiation fiber.

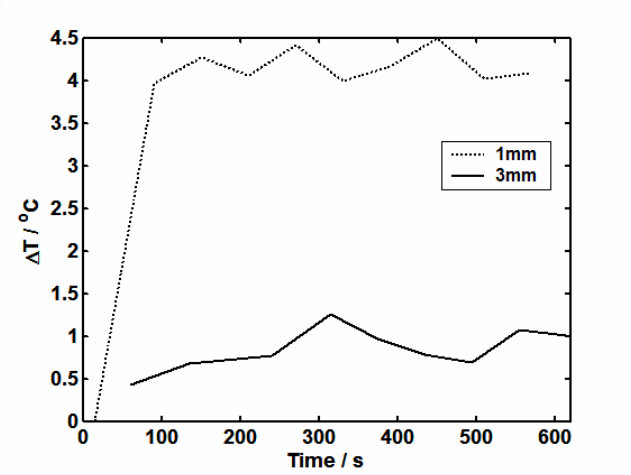

Figure 8. *The measured temperature increase at two different fiber separations.*

An infrared image is shown after 5 minutes of a superficial treatment on skin (Figure 9). The same figure presents a graph of the temperature increase as a function of distance in the infrared image. As can be seen, the increase is about 4 °C close to the middle. This is in good agreement with the measured temperature increase for 1 mm interfiber distance presented in Figure 8. Further out the increase is not of that high value. This shows how important it is to monitor the temperature in the right location.

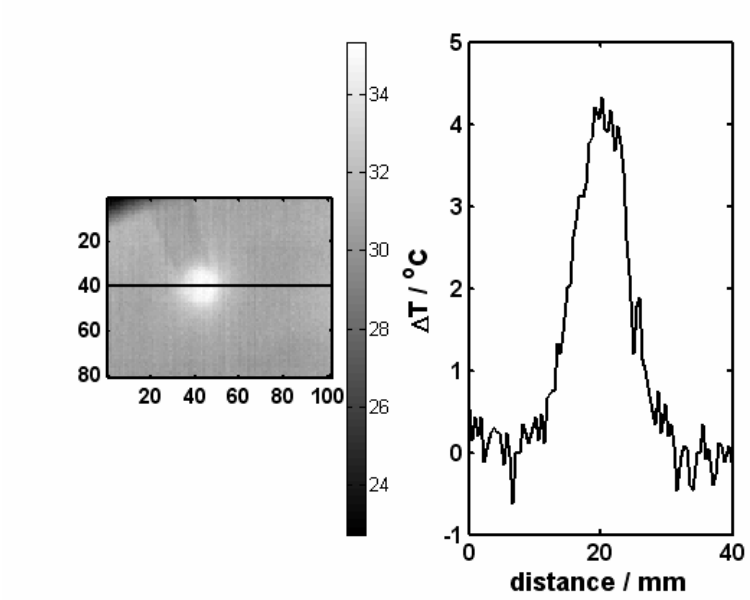

Figure 9. *An infrared image is shown 300 seconds after the start of a superficial treatment on skin (left). The temperature increase is shown as a function of distance (right). The solid line in the left image corresponds to the cross section showed in the right graph.*

To investigate the effect of illumination power on the monitored temperature, illumination with two different powers were utilized. By using the fiber arrangement in Figure 5b, the illumination fiber was the same as the doped fiber used for the measurements, meaning that the local temperature was monitored just where the illumination fiber was located.

The results of these measurements are presented in Figure 10. As it is shown, the temperature increase is larger when using the power of 110 mW compared to a power of 75 mW. This is not an unexpected behaviour when more energy is delivered to the tissue with a higher power. Another interesting feature is that the temperature increase is stabilized after 3 minutes for the power of 75 mW and after 4 minutes with the power of 110 mW, and for the rest of the treatment the temperature is rather constant. This can be explained by a balance between energy deposition due to light absorption and energy dissipation mainly due to the local blood flow. If the increase, as can be seen in the graph, is about 2-4 °C, the blood perfusion will often locally increase to the vicinity of the irradiation position to remove some of the extra heat. It takes approximately 3-4 minutes before the steady state condition is reached in this case. The laser illumination was stopped after 10 minutes, while a few extra temperature measurements were performed to see how the temperature was decreasing. It seems like the temperature decreased even below the initial temperature. An explanation to this may be the expected increased blood perfusion in the area stimulated by the procedure, yielding a slightly different steady state temperature. Only a few minutes after the treatment was interrupted, it seems like the temperature is stabilizing again and will probably approach the initial temperature after a short while when the blood perfusion is back on the normal level. A change in the blood perfusion to the initial perfusion will probably take a few minutes. The reason that the temperature increase is shown instead of an absolute temperature, is that there is a difference in the initial temperatures on different locations of the skin.

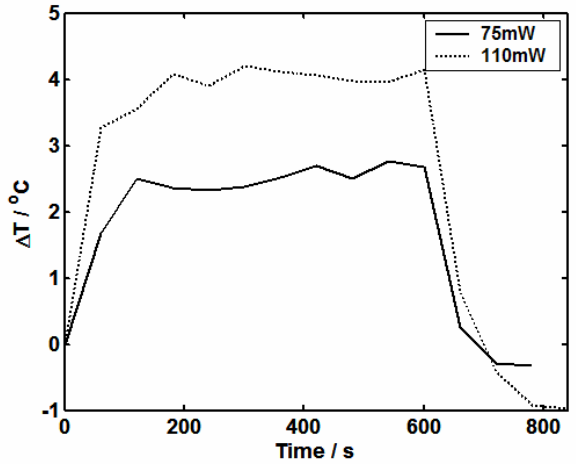

Figure 10. *The temperature as a function of time conducted at two different powers, 75 and 110 mW.*

In another series of measurements on a piece of meet, the temperature increase during an interstitial treatment was monitored. The results of these measurements are shown in Figure 11. Three different curves are corresponding to three different simulated treatment sessions. Two of the treatments were conducted for 10 minutes and one for 20 minutes, while the illumination power and depth of the irradiation were slightly different for the three series of measurements. As can be seen in the graph, the temperature is increasing during the whole session. This can be compared to the superficial measurements on skin where the temperature increase is stabilized after a few minutes as the blood perfusion constitutes the major heat drainage. During interstitial irradiation in meat without any

convection or blood perfusion, the main spread of the heat is due to heat conduction. Heat conduction has a much longer time constant and the temperature will not stabilize for a long time, and at a much higher temperature. The measurements on meat symbolise thus no entirely realistic scenario because of the lack of tissue perfusion. Interestingly though, the temperature increase for the first few hundred seconds are in the same range as in the irradiation of skin.

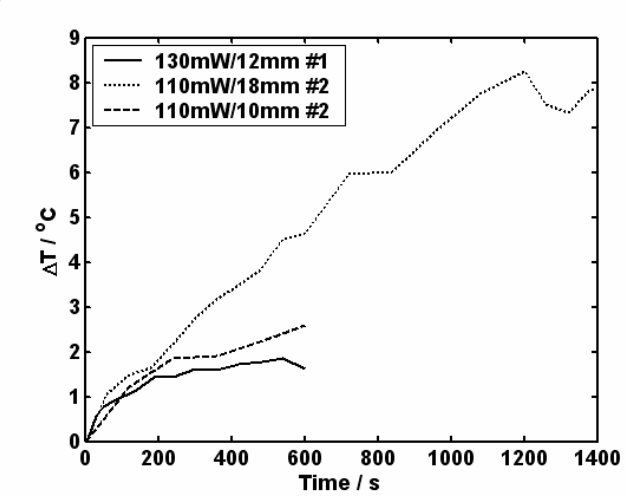

Figure 11. *The temperature increase for three different interstitial treatments performed in a piece of meat. The power/depth and the arrangement used are shown in the legend.*

While PDT is known as a method for treating superficial tumors[37], interstitial treatments may be necessary for the case of thick and/or deep-lying tumors. In this treatment modality a number of optical fibers are inserted into the tumor mass to facilitate the light delivery, and hence, the treatment of thicker and deeper located tumors[13]. Considering the high light fluence rate close to the source fibers, tissue may be heated sufficiently much to locally cause thermal damage. This hypothesis has been investigated in this study, by monitoring the temperature changes in tissue during simulated IPDT treatment on healthy skin and in tissue phantoms. It is of importance that any temperature changes during IPDT is understood and considered in the treatment dosimetry. Temperature alteration may affect the treatment through different mechanisms as discussed in the introduction[38]. It may also be of interest to know if the treatment is purely because of the IPDT or the thermal effects are involved[39]. If the temperature effects become dominant, another modality called *Interstitial Thermotherapy*, comes to the picture. This method denotes the local elevation of temperature within tissues to a level where cell death is enabled[40]. In this method, heat is delivered to tissues through the absorption of light, and the rise in temperature results in a well-defined region of necrosis[41]. In thermotherapy, tissue temperature has to be raised to 50 °C and over, in which the coagulation of tissue occurs[42]. Tissue temperature increased to 46 °C is defined as hyperthermia[43], in which tumor tissue is believed to be more sensitive to heat than normal tissue, hence, hyperthermia is used in a way to cause selective tumor cell death[38].

4. Conclusions

In this study we have shown that tissue temperature can be measured with an optical technique based on the detection of temperature dependent fluorescence light from alexandrite crystal. Simulations of superficial treatments on skin, using a bare cut fiber delivering 110 mW light power at 635 nm, showed that the temperature increase is about 2-4 °C for a treatment of 10 minutes. After 3-4 minutes the temperature remains almost constant. The short period of an abrupt temperature increase is most likely due to the blood perfusion acting as a cooling agent, stabilizing the temperature[40]. Therefore, the range of the temperature increase achieved in this study is so low, suggesting that no thermal effects will interfere with the outcome of IPDT treatment. The conducted simulations of interstitial treatment in meat, has shown the similar temperature increase, but continuing through the entire treatment. In these cases, an increase was shown for the whole treatment, as no blood flow existed in the meat. Studies on the two different fiber arrangements used for treatment, have shown that the fiber arrangement B in Figure 5, where the illumination fiber is crystal doped, is the best for monitoring the local temperature at the fiber tip, since the temperature is monitored exactly at the fiber tip where a high fluence rate is located. It must be mentioned that the big temperature increase will only occur in a distance of a few hundred micrometers from the tip of the illumination fiber[9].

Future work in the project involves more temperature measurements on simulated superficial treatments on volunteers to get a better statistics. Also more interstitial measurements in meat will be conducted. The robustness of the attachment of the crystal to the fiber tip is also an urgent question to be solved. So far, we have seen that only using glue to attach the crystal is not enough, since the fiber tip becomes very fragile.

Acknowledgments

The authors would like to thank Nina Reistad, for supplying an infrared camera, and Lars Wallman, for supplying us with an oven, used for calibration of fiber. The financial support by the company SpectraCure AB and the Swedish Strategic Research Foundation (SSF) are gratefully acknowledged.

References

1. N.Lange, P.Jichlinski, M.Zellweger, M.Forrer, A.Marti, L.Guillou, P.Kucera, G.Wagnieres and B.H.van den, Photodetection of early human bladder cancer based on the fluorescence of 5-aminolaevulinic acid hexylester-induced protoporphyrin IX: a pilot study, *Br. J. Cancer* **80**, 185-193 (1999).

2. J.C.Kennedy, R.H.Pottier and D.C.Pross, Photodynamic therapy with endogenous protoporphyrin IX: Basic principles and present clinical experience, *J. Photochem. Photobiol. B.* **6**, 143-148 (1990).

3. J.C.Kennedy and R.H.Pottier, Endogenous protoporphyrin IX, a clinically useful photosensitizer for photodynamic therapy, *J. Photochem. Photobiol. B.* **14**, 275-292 (1992).

4. A.Castellani, G.P.Pace and M.Concioli, Photodynamic effect of haematoporphyrin on blood circulation, *J. Path. Bact.* **86**, 99-102 (1963).

5. S.S.Stylli, M.Howes, L.MacGregor, P.Rajendra and A.H.Kaye, Photodynamic therapy of brain tumours: evaluation of porphyrin uptake versus clinical outcome, *J. Clin. Neurosci.* **11**, 584-596 (2004).

6. M.J.Niedre, C.S.Yu, M.S.Patterson and B.C.Wilson, Singlet oxygen luminescence as an in vivo photodynamic therapy dose metric: validation in normal mouse skin with topical amino-levulinic acid, *Br. J. Cancer* **92**, 298-304 (2005).

7. P.J.Muller and B.C.Wilson, Photodynamic therapy of malignant brain tumours, *Can. J. Neurol. Sci.* **17**, 193-198 (1990).

8. K.Svanberg, T.Andersson, D.Killander, I.Wang, U.Stenram, S.Andersson-Engels, R.Berg, J.Johansson and S.Svanberg, Photodynamic therapy of non-melanoma malignant tumours of the skin using topical δ-aminolevulinic acid sensitization and laser irradiation, *Br. J. Dermatol.* **130**, 743-751 (1994).

9. I.Wang, N.Bendsoe, C.af Klinteberg, A.M.K.Enejder, S.Andersson-Engels, S.Svanberg and K.Svanberg, Photodynamic therapy versus cryosurgery of basal cell carcinomas; results of a phase III randomized clinical trial, *Br. J. Dermatol.* **144**, 832-840 (2001).

10. G.Jori, Tumour photosensitizers: approach to enhance the selectivity and efficiency of photodynamic therapy, *J. Photochem. Photobiol. B.* **36**, 87-93 (1996).

11. M.Soto Thompson, L.Gustafsson, S.Pålsson, N.Bendsoe, M.Stenberg, C.af Klinteberg, S.Andersson-Engels and K.Svanberg, Photodynamic therapy and diagnostic measurements of basal cell carcinomas using esterified and non-esterified ä-aminolevulinic acid, *J. Porphyrins Phthalocyanines* **5**, 147-153 (2001).

12. M.Stenberg, M.Soto Thompson, T.Johansson, S.Pålsson, C.af Klinteberg, S.Andersson-Engels, U.Stenram, S.Svanberg and K.Svanberg, Interstitial photodynamic therapy- Diagnostic measurements and treatment in malignant experimental rat tumours, in *Optical Biopsy and Tissue Optics*, eds. I.J.Bigio, G.J.Mueller, G.J.Puppels, R.W.Steiner and K.Svanberg, Proc. SPIE vol. **4161**, 151-157 (2000).

13. M.Soto Thompson, A.Johansson, T.Johansson, S.Andersson-Engels, N.Bendsoe, K.Svanberg and S.Svanberg, Clinical system for interstitial photodynamic therapy with combined on-line dosimetry measurements, *Appl. Opt.* **44**, 4023-4031 (2005).

14. J.P.A.Marijnissen, J.A.C.Versteeg, W.M.Star and W.L.J.van Putten, Tumor and normal response to interstitial photodynamic therapy of the rat R-1 rhabdomyosarcoma, *Int. J. Radiat. Oncol. Biol. Phys.* **22**, 963-972 (1992).

15. S.F.Purkiss, R.Dean, J.T.Allardice, M.Grahn and N.S.Williams, An interstitial light delivery system for photodynamic therapy within the liver, *Lasers Med. Sci.* **8**, 253-257 (1993).

16. T.J.Dougherty, R.E.Thoma, D.G.Boyle and K.R.Weishaupt, Interstitial photoradiation therapy for primary solid tumors in pet cats and dogs, *Cancer Res.* **41**, 401-404 (1981).

17. J.P.A.Marijnissen, J.A.C.Versteeg, W.M.Star and W.L.J.Vanputten, Tumor and normal tissue-response to interstitial photodynamic therapy of the rat R-1 rhabdomyosarcoma, *International Journal of Radiation Oncology biology physics* **22**, 963-972 (1992).

18. T.Johansson, M.Soto Thompson, M.Stenberg, C.af Klinteberg, S.Andersson-Engels, S.Svanberg and K.Svanberg, Feasibility study of a novel system for combined light dosimetry and interstitial photodynamic treatment of massive tumors, *Appl. Opt.* **41**, 1462-1468 (2002).

19. C.P.Lowdell, D.V.Ash, I.Driver and S.B.Brown, Interstitial photodynamic therapy. Clinical experience with diffusing fibres in the treatment of cutaneous and subcutaneous tumours, *Br. J. Cancer* **67**, 1398-1403 (1993).

20. T.J.Vogl, K.Eichler, M.G.Mack, S.Zangos, C.Herzog, A.Thalhammer and K.Engelmann, Interstitial photodynamic laser therapy in interventional oncology, *Eur. Radiol.* **14**, 1063-1073 (2004).

21. J.W.Pickering, S.Bosman, P.Posthumus, P.Blokland, J.F.Beek and M.J.C.van Gemert, Changes in the optical properties (at 632.8 nm) of slowly heated myocardium, *Appl. Opt.* **32**, 367-371 (1993).

22. W.M.Star, B.C.Wilson and M.S.Patterson, Light delivery and optical dosimetry in photodynamic therapy of solid tumors, in *Photodynamic Therapy,* ed. B.W.Henderson, pp. 335-367 (New York; Basel; Hong Kong, 1992).

23. L.O.Svaasand, Photodynamic and photohyperthermic response of malignant tumors, *Med. Phys.* **12**, 455-461 (1985).

24. I.J.Bigio and S.G.Bown, Spectroscopic sensing of cancer and cancer therapy - Current status of translational research, *Cancer Biology & Therapy* **3**, 259-267 (2004).

25. I.J.Bigio and J.R.Mourant, Ultraviolet and visible spectroscopies for tissue diagnostics: fluorescence spectroscopy and elastic-scattering spectroscopy, *Phys. Med. Biol.* **42**, 803-814 (1997).

26. S.Pålsson, L.Gustafsson, N.Bendsoe, M.Soto Thompson, S.Andersson-Engels and K.Svanberg, Kinetics of the superficial perfusion and temperature in connection with photodynamic therapy of basal cell carcinomas using esterified and non-esterified 5-aminolevulinic acid, *Br. J. Dermatol.* **148**, 1179-1188 (2003). English.

27. W.M.A.Niessen and J.Van Der Greef, *Liquid Chromatography-Mass Spectrometry: Principles and Applications*, (Marcel Dekker, 1992).

28. S.Gucg Jr. and C.E.Jones, Alexandrite-laser performance at high temperature, *Opt. Lett.* **7**, 608-610 (1982).

29. W.B.White, R.R.Roy and J.M.Crichton, The "alexandrite effect": and optical study., *American Mineralogist* **52**, 867-871 (1967).

30. C.P.Poole, The optical spectra and color of chromium containing solids., *Journal of Physics and Chemistry of Solids* **25**, 1169-1182 (1964).

31. L.R.Bernstein, Monazite from North Carolina having the alexandrite effect, *American Mineralogist* **67**, 356-359 (1982).

32. K.T.V.Grattan and Z.Y.Zhang, *Fiber optic fluorescence thermometry*, (Chapman & Hall, London, 1995).

33. R.C.Powell, L.Xi, X.Gang, G.J.Quarles and J.C.Walling, Spectroscopic properties of alexandrite crystals, *Physical Review B* **32**, 2788-2797 (1985).

34. J.Svensson, A.Ralsgård, T.Johansson and S.Andersson-Engels, Tissue temperature measurements during interstitial laser therapy using Cr^{3+}-doped crystals at the fiber tip, *Therapeutic Laser Applications and Laser-Tissue Interactions* **5142**, 30-41 (2004).

35. J.Wren, Evaluation of three temperature measurement methods used during microwave thermotherapy of prostatic enlargement, *Int. J. Hyperthermia* **20**, 300-316 (2004).

36. J.R.Mourant, I.J.Bigio, D.A.Jack, T.M.Johnson and H.D.Miller, Measuring absorption coefficients in small volumes of highly scattering media: source-detector separations for which path lengths do not depend on scattering properties, *Appl. Opt.* **36**, 5655-5661 (1997).

37. S.B.Brown, E.A.Brown and I.Walker, The present and future role of photodynamic therapy in cancer treatment, *Lancet Oncology* **5**, 497-508 (2004).

38. L.E.Gerweck, Hyperthermia in cancer therapy: the biological basis and unresolved questions, *Cancer Res.* **45**, 3408-3414 (1985).

39. P.H.Möller, P.H.Hannesson, K.Ivarsson, J.Olsrud, U.Stenram and K.G.Tranberg, Interstitial laser thermotherapy in pig liver: effect of inflow occlusion on extent of necrosis and ultrasound image, *Hepato-gastroenterol.* **44**, 1302-1311 (1997).

40. K.Ivarsson, J.Olsrud, C.Sturesson, P.H.Möller, B.R.Persson and K.-G.Tranberg, Feedback interstitial diode laser (805 nm) thermotherapy system: ex vivo evaluation and mathematical modeling with one and four-fibers, *Lasers Surg. Med.* **22**, 86-96 (1998).

41. S.G.Bown, Phototherapy of tumours, *World J. Surg.* **7**, 700-709 (1983).

42. C.Sturesson, Medical laser-induced thermotherapy- models and applications, Dissertation thesis, Lund Institute of Technology, Lund, Sweden (1998).

43. J.Eichler, J.Leibetruth, R.A.London and L.Ziegenhagen, Temperature distribution for combined laser hyperthermia–photodynamic therapy in the esophagus, *Medical Engineering & Physics* **22**, 307-312 (2000).